الحل المرن للإجهاد في نفق توأم
عميق على أساس نظرية المتغير المركب ومبدأ التراكب

جيو ذي—هونغ * ، ليو شين—رونغ** وزهو زهانيوان***

* كلية الهندسة المدنية، جامعة سيتشوان الزراعية، سيتشوان، دوجيانغيان 611830، الصين

** كلية الهندسة المدنية، جامعة تشونغتشينغ، تشونغتشينغ 400045، الصين

*** هيئة سيتشوان العليا لمركز البحوث الهندسية للحد واتقاء الكوارث، دوجيانغيان، 611830، الصين

الخـلاصـة

نظرية المتغير المركب ومبدأ التراكب طرق مفيدة لدراسة النفق الإجهاد والتشوه. وبناء على ذلك، يرد حلاً مرناً لتوزيع الإجهاد نفق التوأمين في الصخور متجانس وموحد الخواص يتعرضون للإجهاد غير موحدة. آخذا في الاعتبار تأثيرات الضغط الداعمة، وتباعد المسافة ومعامل الإجهاد، يتم تطبيق الحل مطاطا والأسلوب عنصر لانهائية لتحليل توزيع الإجهاد النفق التوأم وتركيز. تظهر النتائج أن أقصى إجهاد النفق التوأم يظهر عند الحائط المتوسطة الصخرة، وتباعد المسافة لها تأثير أكثر وضوحاً على تركيز الإجهاد. الفرق أكبر في توزيع الإجهاد بين الحل التحليلي وطريقة العناصر المحدودة في هانسيس النفق التوأم الأيمن والأيسر، ولكن البيانات التحليلية الغاية متسقة مع البيانات العددية. ومع ذلك، قد تصبح الفرق كبير إذا كان تباعد المسافة النفق التوأم أقل من 0.25 مرات قطر النفق ومعامل الإجهاد أقل من 0.7.

Elastic Solution for a Deep Twin Tunnel's Stress Based on Complex Variable Theory and the Superposition Principle

Guo Zi-hong*, Liu Xin-rong** and Zhu Zhanyuan***

* *College of Civil Engineering, Sichuan Agricultural University, Sichuan, Dujiangyan, 611830, China*

** *College of Civil Engineering, Chongqing University, Chongqing 400045, China,*

*** *Sichuan Higher Institution Engineering Research Center of Rural Construction Disaster Prevention and Reduction, Dujiangyan, 611830, China,*

* *Corresponding Author: guozihonghyx@sicau.edu.cn*

ABSTRACT

Complex variable theory and the superposition principle are useful ways to study a tunnel's stress and deformation. Accordingly, an elastic solution is presented for a twin tunnel's stress distribution in homogeneous and isotropic rock subjected to non-uniform stress. Taking into account the influences of the supporting pressure, spacing distance and stress coefficient, the elastic solution and infinite element method are applied to analyze the twin tunnel's stress distribution and concentration. The results demonstrate that the twin tunnel's maximum stress appears at the middle rock wall, and the spacing distance has most evident influence on the stress concentration. The largest difference in the stress distribution between the analytical solution and the finite element method is at the twin tunnel's left and right hances, but the analytical data are highly consistent with the numerical data. Nevertheless, the difference may become significant if the twin tunnel's spacing distance is less than 0.25 times the tunnel diameter and the stress coefficient is less than 0.7.

Keywords: Complex variable theory; deep twin tunnel; elastic solution; stress distribution; superposition principle.

INTRODUCTION

Tunnels, as a main way to utilize underground space, play a highly important role in infrastructure. The field of tunnel engineering has greatly blossomed, attracting the attention of engineers. A tunnel's stress distribution and deformation are critical factors to evaluate its stability, so most researchers have focused on the tunnel's stress distribution and displacement. Pender (1980) presented elastic solutions for a deep circular tunnel in a non-uniform stress field to analyze the displacement and stress distribution.Park (2004) presented elastic solutions for the prediction of tunneling-induced ground deformations for shallow and deep tunnels in soft ground. An analytical solution is presented to predict the stresses and displacements of a circular tunnel in a Mohr–Coulomb rock mass subjected to hydrostatic stress (Wang et al., 2012).Based on elastic theory and the transfer matrix technique, Sulem et al. (2013) analyzed the stresses and displacements in a two-dimensional circular opening excavated in a transversely isotropic formation with nonlinear behavior.

When considering a tunnel with an arbitrary sectionand non-uniform loading boundary, complex variable functionsare very helpful.Complex variable theory has been employed to find the analytical solution for the rock stress around square tunnels in a homogeneous, isotropic and elastic rock mass (Zhao & Yang, 2015), the solution for deep lined circular tunnels in transversely anisotropic rock (Bobet, 2016), a closed-form elastic solution for stresses and displacements around a tunnel with an arbitrary section (Exadaktylos & Stavropoulou, 2002), and the stress solution for a lined non-circular tunnel subjected to a uniform ground load (Kargar et al., 2014). Based on complex variables, the analytic stress solution for a circular pressure tunnel at great pressure and depth including support delay (Lü et al., 2011; Carranza-Torres et al., 2013) and the solution of a tunnel in a homogeneous and isotropic material taking the construction sequence and support delay into account (Li & Wang, 2008)are presented.

With complex variable theory, ashallow tunnel in a half-plane can be changed into a circular ring, so that the shallow tunnel's stress and displacement can be solved (Verruijt, 1998; Strack & Verruijt,2002).A solution for plane containing two holes is presented (Ling., 1948). Fu et al. (2015) analyzeda twin tunnel's deformationusing superposition principle. The Schwarz alternating method was used to analyze a twin tunnel's stress through simplifying a multiply connected region to a single-connected region, and it is necessary that the iteration number should be increased to enhance the analytical accuracy. (Yan et al., 2011; Kooi & Verruijt, 2001; Su et al., 2012).A closed-form solution is presented for the stresses and displacements around two deep circular tunnels (Tran-Manh et al., 2015).

Based on complex variable theory and the superposition principle, an elastic solution is presented to analyze a twin circular tunnel in homogeneous and isotropic rock on the condition of a non-uniform stress field.The influences of the supporting pressure, spacing distance and stress coefficient on the stress distribution are discussed. The finite element method is applied to study the twin tunnel's stress distribution, and the result is compared with the analytical solution. The elastic solution validated by the finite element method can quickly describe the twin tunnel's stress distribution at another angle.

SIMPLIFICATION OF THE TWIN TUNNEL'S STRESS FIELD

When a twin tunnel is built at great depth, the influence of gravity near the tunnel is very unobvious. Hence, engineers often only take the vertical stress (q_v) and horizontal stress (q_h) into account to analyze a deep tunnel's stress field, as shown in Figure 1. The stress coefficient is defined as q_h/q_v.The stress superposition principle is very helpful to simplify the engineering calculations. Based on stress superposition, the Schwarz alternating method was used to analyze the twin tunnel's stress, with a single-connected region used to solve problems of a multiply connected region (Kooi & Verruijt, 2001; Zhang et al., 2000). Hence, the twin tunnel's stress field in Figure 1 can be changed into the sum of stress fields shown in Figure 2, namely, the sum of the initial stress field and stress field under q(x, y), where q_0 is the supporting pressure and q(x, y) equals the initial stress field minus the supporting pressure q_0.
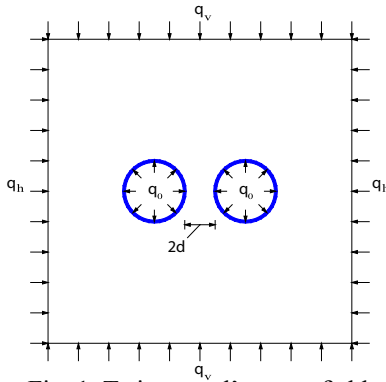
Fig. 1. Twin tunnel's stress field
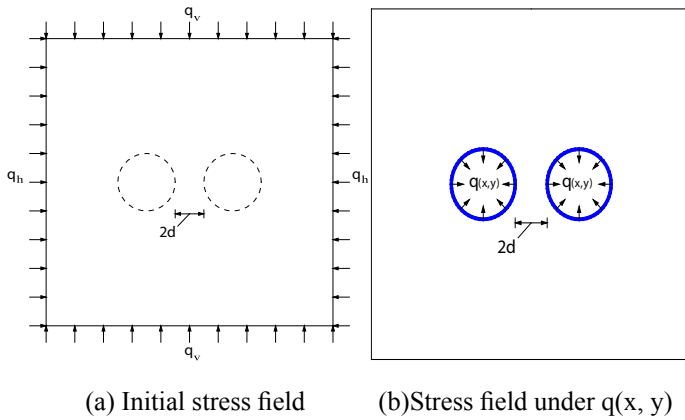
(a) Initial stress field   (b)Stress field under q(x, y)

Fig. 2. Analysis of twin tunnel's stress field

It is clear that analyzing the stress distribution in a multiply connected region is more difficult than in a single-connected region. Because of the symmetry of the structure and load, the stress field in Figure 2 (b) can be redrawn as a half-plane stress field with a circular tunnel in Figure3, where A is the origin point (0, 0), h is the horizontal distance between the origin point and the tunnel's center, and d is the horizontal distance from the origin point to the tunnel's left hance (half the spacing distance of the twin tunnel).
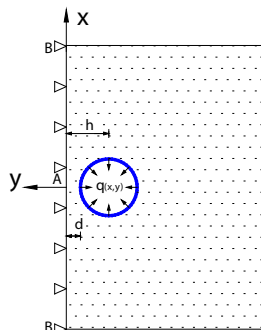
Fig. 3. Half-plane stress field with circular tunnel

ELASTIC METHOD WITH COMPLEX VARIABLE FUNCTION

The elastic mechanics of the complex variable function allows the solution of the elastic plane problem to be expressed by the complex stress functions $\phi(z)$ and $\psi(z)$, which are analytic everywhere in the half plane with the exclusion of the circular tunnel. The relationship between the stress and complex stress functions can be defined by following equations:

$$\sigma_x + \sigma_y = 2\left\{\phi'(z) + \overline{\phi'(z)}\right\} = 4\,\mathrm{Re}\left\{\phi'(z)\right\} \tag{1}$$

$$\sigma_y - \sigma_x + 2i\tau_{xy} = 2\left\{\overline{z}\phi''(z) + \psi'(z)\right\} \tag{2}$$

The relationship betweenthe displacement and the complex stress functions can be defined by

$$2G\left(u_x + iu_y\right) = k_\mu\phi(z) - z\overline{\phi'(z)} - \overline{\psi(z)} \tag{3}$$

where G is the shear modulus of the surrounding rock, $G = E/2(1+\mu)$, is Poisson's ratio, E is the elastic modulus, and k_μ is a parameter that is related to Poisson's ratio, $k_\mu = 3 - 4\mu$ for a for a plane strain.

The stress boundary conditions are expressed by a complex variable function, and the integral of the force along the boundary conditions is defined by

$$F(s) = F_1 + iF_2 = i\int_{s0}^{s}\left(X_n + iY_n\right)ds \tag{4}$$

The displacement and stress boundary conditions ofa half-plane with a circular tunnel in Figure 3 are obtained by

$$y = 0: \begin{cases} 2iGu_y = \mathrm{Im}\left\{k_\mu\phi(z) - z\overline{\phi'(z)} - \overline{\psi(z)}\right\} = C_1 \\ i\tau_{xy} = \mathrm{Im}\left\{\overline{z}\phi''(z) + \psi'(z)\right\} = 0 \end{cases} \tag{5}$$

$$x^2 + (y+h)^2 = r^2 : \phi(z) + z\overline{\phi'(z)} + \overline{\psi(z)} = F(s) + C_2 \tag{6}$$

where X_n is the stress in the X-direction, Y_n is the stress in the Y-direction, s_0 is an arbitrary point on the boundary, and C_1 and C_2 are unknown constants.

Stress and mapping function

A half-plane with a circular tunnel in the Z plane can be mapped into a ring region M in the z plane in Figure 4. Region M consists of an outer circle of $|\zeta| = 1$ and an inner circle of $|\zeta| = \alpha$. Verruijt (1998) chose Equation (7) as the mapping function to analyze the half-plane problem with a circular hole.
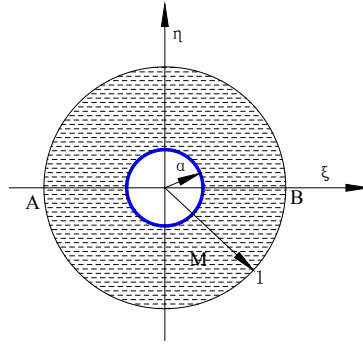
Fig. 4. Ring region in ζ plane

$$z = \omega(\zeta) = -ih\frac{1-\alpha^2}{1+\alpha^2}\frac{1+\zeta}{1-\zeta} \tag{7}$$

where $0 < \alpha < 1$. α.is a parameter, defined by r/h. Their relationship can be described as

$$\frac{r}{h} = \frac{2\alpha}{1+\alpha^2} \tag{8}$$

Each distinct point in theplane corresponds to a distinctpoint in the Z plane. The boundary of $|\zeta|=1$ corresponds to the axis y=0, the boundary of $|\zeta|=\alpha$ corresponds to the circle $x^2 +(y+h)^2 = r^2$, the Z plane's origin corresponds to $\zeta = -1$, and the Z plane's infinite point corresponds to $\zeta = 1$. If $\alpha \to 0$, the horizontal distance from the circle's center to theX-axis is very large, so the twin tunnel's space is very large. If $\alpha \to 1$, the radius of the circular tunnel is close to the horizontal distance from the circle's center to the X-axis, which means that the spacing distance between the two tunnels is close to zero. Every corresponding value of ζ can be defined by Equation (7).

The mapping function $\omega(\zeta)$ is an analytic function in the ring region M of the ζ plane. The complex functions $\phi(z)$ and $\psi(z)$ are also analytic functions in the R region of the Z plane. The complex stress function can be rewritten as

$$\phi(z) = \phi(\omega(\zeta)) = \phi_1(\zeta) = \sum_{k=0}^{\infty} a_k\zeta^k + \sum_{k=1}^{\infty} b_k\zeta^{-k} \tag{9}$$

$$\psi(z) = \psi(\omega(\zeta)) = \psi_1(\zeta) = \sum_{k=0}^{\infty} c_k\zeta^k + \sum_{k=1}^{\infty} d_k\zeta^{-k} \tag{10}$$

Because the stress only exists in the boundary of the circular tunnel, the stress and displacement of the infinite distance are close to zero. The coefficients a_k, b_k, c_k and d_k are determined by the boundary conditions. Equation(5)and(6)are boundary conditions that contains $\phi(z)$, $\psi(z)$, $\phi'(z)$, $\psi'(z)$ and $\phi''(z)$, and ζ can be written as

$$\phi'(z) = \frac{d\phi_1(\zeta)}{dz} = \frac{d\phi_1(\zeta)}{d\zeta}\frac{d\zeta}{dz} = \frac{\phi_1'(\zeta)}{\omega'(\zeta)} \tag{11}$$

$$\psi'(z) = \frac{d\psi_1(\zeta)}{dz} = \frac{d\psi_1(\zeta)}{d\zeta}\frac{d\zeta}{dz} = \frac{\psi_1'(\zeta)}{\omega'(\zeta)} \tag{12}$$

$$\phi''(z) = \frac{d\phi_1'(\zeta)}{dz} = \frac{d\phi_1'(\zeta)}{d\zeta}\frac{d\zeta}{dz} = \left[\phi_1''(\zeta)\omega'(\zeta) - \phi_1'(\zeta)\omega''(\zeta)\right]/\left[\omega'(\zeta)\right]^3 \tag{13}$$

$$z\overline{\phi'(z)} = \frac{\omega'(\zeta)}{\overline{\omega'(\zeta)}}\overline{\phi_1'(\zeta)} \tag{14}$$

$$\overline{z}\phi''(z) = [\frac{\overline{\omega(\zeta)}}{\omega'(\zeta)}\phi_1''(\zeta) - \frac{\overline{\omega(\zeta)}}{\omega'(\zeta)}\frac{\omega''(\zeta)}{\omega'(\zeta)}\phi_1'(\zeta)]/\omega'(\zeta) \tag{15}$$

$$\omega'(\zeta) = -2ih\frac{1-\alpha^2}{1+\alpha^2}\frac{1}{(1-\zeta)^2} \tag{16}$$

$$\omega''(\zeta) = -4ih\frac{1-\alpha^2}{1+\alpha^2}\frac{1}{(1-\zeta)^3} \tag{17}$$

$$\frac{\omega'(\zeta)}{\overline{\omega'(\zeta)}} = -\frac{(1+\zeta)(1-\overline{\zeta})^2}{2(1-\zeta)} \tag{18}$$

$$\frac{\omega''(\zeta)}{\omega'(\zeta)} = \frac{2}{1-\zeta} \tag{19}$$

To analyze the stress distribution of the half-plane with a circular tunnel in the Z plane, some coefficients should be simplified by conformal transformation mapping in ring region M of the ζ plane. A ring with a radius of ρ can be expressed as $\zeta = \rho\sigma$ and $\overline{\zeta} = \rho\sigma^{-1}$, where $\sigma = \exp(i\theta)$, so that Equations (18) and (19)can be rewritten as

$$\frac{\omega(\zeta)}{\overline{\omega'(\zeta)}} = -\frac{1}{2}\frac{(1+\rho\sigma)(\sigma-\rho)^2}{\sigma^2(1-\rho\sigma)} \tag{20}$$

$$\frac{\omega''(\zeta)}{\omega'(\zeta)} = \frac{2}{1-\rho\sigma} \tag{21}$$

Boundary conditions at X-axis

The circle of $|\zeta| = 1$ in the ζ plane corresponds to the X-axis, so Equation (5) is rewritten as

$$\mathrm{Im}\left\{k_\mu\phi_1(\zeta) - \frac{\omega(\zeta)}{\overline{\omega'(\zeta)}}\overline{\phi_1'(z)} - \overline{\psi_1(z)}\right\} = C_1 \tag{22}$$

$$\mathrm{Im}\left\{\left[\frac{\overline{\omega(\zeta)}}{\overline{\omega'(\zeta)}}\phi_1''(z) - \frac{\overline{\omega(\zeta)}}{\overline{\omega'(\zeta)}}\frac{\omega''(\zeta)}{\omega'(\zeta)}\phi_1'(z) + \psi_1'(z)\right]/\omega'(\zeta)\right\} = 0 \tag{23}$$

Equations (20) and (21) can be simplified as

$$\frac{\omega(\zeta)}{\overline{\omega'(\zeta)}} = \frac{1}{2}(1-\sigma^2); \quad \frac{\omega''(\zeta)}{\omega'(\zeta)} = \frac{2}{1-\sigma} \tag{24}$$

$k_\mu\phi_1(\zeta) - \dfrac{\omega(\zeta)}{\overline{\omega'(\zeta)}}\overline{\phi_1'(z)} - \overline{\psi_1(z)} = f_1$ is defined, and then

$$\begin{aligned}
f_1 &= \sum_{k=1}^{\infty}k_\mu a_k\sigma^k + \frac{1}{2}\sum_{k=1}^{\infty}(k-1)\bar{b}_{k-1}\sigma^k - \frac{1}{2}\sum_{k=1}^{\infty}(k+1)\bar{b}_{k+1}\sigma^k - \sum_{k=1}^{\infty}\bar{d}_k\sigma^k + \sum_{k=1}^{\infty}k_\mu b_k\sigma^{-k} \\
&- \frac{1}{2}\sum_{k=1}^{\infty}(k+1)\bar{a}_{k+1}\sigma^{-k} + \frac{1}{2}\sum_{k=1}^{\infty}(k-1)\bar{a}_{k-1}\sigma^{-k} - \sum_{k=1}^{\infty}\bar{c}_k\sigma^{-k} + k_\mu a_0 - \bar{c}_0 - \frac{\bar{b}_1}{2} - \frac{\bar{a}_1}{2}
\end{aligned} \tag{25}$$

$f_1 - \overline{f_1} = C_1 - \overline{C_1} = C_3$ is clear from Equation(22), where C_3 is a real constant, and the equation can be expressed as

$$\begin{aligned}
&\sum_{k=1}^{\infty}\sigma^k\left[k_\mu a_k + \frac{1}{2}(k-1)\bar{b}_{k-1} - \frac{1}{2}(k+1)\bar{b}_{k+1} - \bar{d}_k - k_\mu\bar{b}_k + \frac{1}{2}(k+1)a_{k+1} - \frac{1}{2}(k-1)a_{k-1} + c_k\right] \\
&- \sum_{k=1}^{\infty}\sigma^{-k}\left[k_\mu\bar{a}_k + \frac{1}{2}(k-1)b_{k-1} - \frac{1}{2}(k+1)b_{k+1} - d_k - k_\mu b_k + \frac{1}{2}(k+1)\bar{a}_{k+1} - \frac{1}{2}(k-1)\bar{a}_{k-1} + \bar{c}_k\right] \\
&- \left(\bar{c}_0 - c_0\right) + k_\mu\left(a_0 - \bar{a}_0\right) - \frac{1}{2}\left(\bar{b}_1 - b_1\right) - \frac{1}{2}\left(\bar{a}_1 - a_1\right) = C_3
\end{aligned} \tag{26}$$

Judging from Equation (28), the sum of the coefficients for each power of σ on both sides should be equal to zero, so every sum of coefficients σ^k or σ^{-k} is zero. Because the coefficient of σ^k is a conjugate complex number of the coefficient of σ^{-k}, the sum of the coefficients of σ^k equals zero when the sum of the coefficients of σ^{-k} equals zero, and the relationships are written as

$$k_\mu \left(a_0 - \bar{a}_0\right) - \left(\bar{c}_0 - c_0\right) - \frac{1}{2}\left(\bar{b}_1 - b_1\right) - \frac{1}{2}\left(\bar{a}_1 - a_1\right) - C_3 = 0 \tag{27}$$

$$\bar{d}_k - c_k = k_\mu a_k + \frac{1}{2}(k-1)\bar{b}_{k-1} - \frac{1}{2}(k+1)\bar{b}_{k+1} - k_\mu \bar{b}_k + \frac{1}{2}(k+1)a_{k+1} - \frac{1}{2}(k-1)a_{k-1} \quad \kappa = 1,2,3,...$$

On the condition of $\dfrac{\overline{\omega(\zeta)}}{\omega'(\zeta)}\phi_1''(z) - \dfrac{\overline{\omega(\zeta)}}{\omega'(\zeta)}\dfrac{\omega''(\zeta)}{\omega'(\zeta)}\phi_1'(z) + \psi_1'(z) = f_2$, the following equation is explicit: (28)

$$f_2 = \frac{1}{2}\sum_{k=1}^\infty k(k-1)a_k\sigma^{k-2} + \frac{1}{2}\sum_{k=1}^\infty k(k+1)b_k\sigma^{-(k+2)} - \frac{1}{2}\sum_{k=1}^\infty k(k-1)a_k\sigma^k - \sum_{k=1}^\infty ka_k\sigma^k$$

$$- \sum_{k=1}^\infty ka_k\sigma^{k-1} + \sum_{k=1}^\infty kb_k\sigma^{-(k+1)} - \frac{1}{2}\sum_{k=1}^\infty k(k+1)b_k\sigma^{-k} + \sum_{k=1}^\infty kb_k\sigma^{-k} + \sum_{k=1}^\infty kc_k\sigma^{k-1} - \sum_{k=1}^\infty kd_k\sigma^{-(k+1)} \tag{29}$$

Judging from Equation (23), it is clear that $f_2\overline{\omega'(\zeta)}$ is equal to $\overline{f}_2\omega'(\zeta)$ so the following equation can be presented:

$$\sigma f_2 + \frac{1}{\sigma}\overline{f}_2 = 0 \tag{30}$$

Equation(30)can be rewritten as

$$\sum_{k=1}^\infty \sigma^k \left[k(k+1)a_{k+1} - (k-1)ka_{k-1} - 2ka_k + 2kc_k + k(k-1)\bar{b}_{k-1} + 2k\bar{b}_k - (k+1)k\bar{b}_{k+1} - 2k\bar{d}_k\right]$$

$$+ \sum_{k=1}^\infty \sigma^{-k}\left[k(k+1)\bar{a}_{k+1} - (k-1)k\bar{a}_{k-1} - 2k\bar{a}_k + 2k\bar{c}_k + k(k-1)b_{k-1} - (k+1)kb_{k+1} + 2kb_k - 2kd_k\right] = 0 \tag{31}$$

where the coefficients' relationship between σ^k and σ^{-k} is also a conjugate complex number. The following equations are available.

$$2k\left(\bar{d}_k - c_k\right) = k(k+1)a_{k+1} - k(k-1)a_{k-1} - 2ka_k + k(k-1)\bar{b}_{k-1} - k(k+1)\bar{b}_{k+1} + 2k\bar{b}_k \quad k = 1,2,3... \tag{32}$$

Boundary condition at tunnel's surface

The surface force along a circular tunnel is expressed by Equation (6) in the Z plane, and it can be rewritten at the boundary $|\zeta| = \alpha$ in the ζ plane

$$\phi_1(\zeta) + \frac{\omega(\zeta)}{\overline{\omega'(\zeta)}}\overline{\phi_1'(\zeta)} + \overline{\psi_1(\zeta)} = F(\zeta) + C_2 \tag{33}$$

where $F(s)$ is determined by the stress boundary condition of a circular tunnel in the Z plane. Any points of $\zeta = \alpha\sigma$ are at the circle boundary of $|\zeta| = \alpha$, so Equation (20) can be simplified to

$$\frac{\omega(\zeta)}{\overline{\omega'(\zeta)}} = \frac{-\alpha\sigma - \left(1 - 2\alpha^2\right) + \alpha\left(2 - \alpha^2\right)\sigma^{-1} - \alpha^2\sigma^{-2}}{2\left(1 - \alpha\sigma\right)} \tag{34}$$

To simplify Equation (33), it can be written as

$$\left(1 - \alpha\sigma\right)\left(\sigma - \alpha\right)\left[\phi_1(\zeta) + \frac{\omega(\zeta)}{\overline{\omega'(\zeta)}}\overline{\phi_1'(\zeta)} + \overline{\psi_1(\zeta)}\right] = \left(1 - \alpha\sigma\right)\left(\sigma - \alpha\right)\left[F(\alpha\sigma) + C_2\right] \tag{35}$$

Where the result of $\left(1 - \alpha\sigma\right)\left(\sigma - \alpha\right)$ is not equal to zero, and

$$F_1(\alpha\sigma) = \left(1 - \alpha\sigma\right)\left(\sigma - \alpha\right)F(\alpha\sigma) \tag{36}$$

The expression of $F_1(\alpha\sigma)$ depends on the boundary condition of the circular tunnel, and $F_1(\alpha\sigma)$ can be written as a Fourier series under the polar coordinate condition:

$$F_1(\alpha\sigma) = \sum_{k=-\infty}^{\infty} A_k\sigma^k \tag{37}$$

The front partsof Equation (35) can be written as

$$\left(1 - \alpha\sigma\right)\left(\sigma - \alpha\right)\phi_1(\zeta) = \left(\sum_{k=0}^{\infty} a_k\alpha^k\sigma^k + \sum_{k=1}^{\infty} b_k\alpha^{-k}\sigma^{-k}\right)\left[-\alpha + \sigma\left(1 + \alpha^2\right) - \alpha\sigma^2\right]$$

$$= -a_0\alpha - a_1\alpha^2\sigma - a_2\alpha^3\sigma^2 - \sum_{k=3}^{\infty} a_k\alpha^{k+1}\sigma^k - \sum_{k=1}^{\infty} b_k\alpha^{1-k}\sigma^{-k} + \left(1 + \alpha^2\right)\left(a_0\sigma + a_1\alpha\sigma^2 + b_1\alpha^{-1}\right. \tag{38}$$

$$\left. + \sum_{k=3}^{\infty} a_{k-1}\alpha^{k-1}\sigma^k + \sum_{k=1}^{\infty} b_{k+1}\alpha^{-1-k}\sigma^{-k}\right) - a_0\alpha\sigma^2 - \sum_{k=3}^{\infty} a_{k-2}\alpha^{k-1}\sigma^k - b_1\sigma - b_2\alpha^{-1} - \sum_{k=1}^{\infty} b_{k+2}\alpha^{-1-k}\sigma^{-k}$$

$$\left(1-\alpha\sigma\right)\left(\sigma-\alpha\right)\overline{\psi_1\left(\zeta\right)} = \left(\sum_{k=0}^{\infty}\overline{c}_k\alpha^k\sigma^{-k} + \sum_{k=1}^{\infty}\overline{d}_k\alpha^{-k}\sigma^k\right)\left[-\alpha+\sigma\left(1+\alpha^2\right)-\alpha\sigma^2\right]$$

$$=\left(1+\alpha^2\right)\left(\overline{c}_0\sigma^1 + \overline{c}_1\alpha + \sum_{k=1}^{\infty}\overline{c}_{k+1}\alpha^{k+1}\sigma^{-k} + \overline{d}_1\alpha^{-1}\sigma^2 + \sum_{k=3}^{\infty}\overline{d}_{k-1}\alpha^{1-k}\sigma^k\right) - \overline{c}_0\alpha - \sum_{k=1}^{\infty}\overline{c}_k\alpha^{k+1}\sigma^{-k} \quad (39)$$

$$-\overline{d}_1\sigma - \overline{d}_2\alpha^{-1}\sigma^2 - \sum_{k=3}^{\infty}\overline{d}_k\alpha^{1-k}\sigma^k - \overline{c}_0\alpha\sigma^2 - \overline{c}_1\alpha^2\sigma - \overline{c}_2\alpha^3 - \sum_{k=1}^{\infty}\overline{c}_{k+2}\alpha^{k+3}\sigma^{-k} - \sum_{k=3}^{\infty}\overline{d}_{k-2}\alpha^{3-k}\sigma^k$$

$$\left(1-\alpha\sigma\right)\left(\sigma-\alpha\right)\frac{\omega\left(\zeta\right)}{\omega'\left(\zeta\right)}\overline{\phi_1'\left(\zeta\right)}$$

$$=\left(1-\alpha\sigma\right)\left(\sigma-\alpha\right)\left[-\frac{1}{2}\frac{\left(1+\alpha\sigma\right)\left(\sigma-\alpha\right)^2}{\sigma^2\left(1-\alpha\sigma\right)}\right]\left(\sum_{k=1}^{\infty}k\overline{a}_k\alpha^{k-1}\sigma^{1-k} - \sum_{k=1}^{\infty}k\overline{b}_k\alpha^{-k-1}\sigma^{k+1}\right)$$

$$= -\tfrac{1}{2}\overline{a}_1\alpha\sigma^2 - \overline{a}_2\alpha^2\sigma - \tfrac{3}{2}\overline{a}_3\alpha^3 - \tfrac{1}{2}\sum_{k=1}^{\infty}\left(k+3\right)\overline{a}_{k+3}\alpha^{k+3}\sigma^{-k} + \tfrac{1}{2}\sum_{k=4}^{\infty}\left(k-3\right)\overline{b}_{k-3}\alpha^{3-k}\sigma^k$$

$$-\tfrac{1}{2}\left(1-3\alpha^2\right)\left(\overline{a}_1\sigma + 2\overline{a}_2\alpha + \sum_{k=1}^{\infty}\left(k+2\right)\overline{a}_{k+2}\alpha^{k+1}\sigma^{-k} - \sum_{k=3}^{\infty}\left(k-2\right)\overline{b}_{k-2}\alpha^{1-k}\sigma^k\right) \quad (40)$$

$$-\tfrac{1}{2}\left(3\alpha^3 - 3\alpha\right)\left(\overline{a}_1 + \sum_{k=1}^{\infty}\left(k+1\right)\overline{a}_{k+1}\alpha^k\sigma^{-k} - \overline{b}_1\alpha^{-2}\sigma^2 - \sum_{k=3}^{\infty}\left(k-1\right)\overline{b}_{k-1}\alpha^{-k}\sigma^k\right)$$

$$-\tfrac{1}{2}\left(3\alpha^2 - \alpha^4\right)\left(\sum_{k=1}^{\infty}k\overline{a}_k\alpha^{k-1}\sigma^{-k} - \overline{b}_1\alpha^{-2}\sigma - 2\overline{b}_2\alpha^{-3}\sigma^2 - \sum_{k=3}^{\infty}k\overline{b}_k\alpha^{-k-1}\sigma^k\right)$$

$$+\tfrac{1}{2}\sum_{k=2}^{\infty}\left(k-1\right)\overline{a}_{k-1}\alpha^{k+1}\sigma^{-k} - \tfrac{1}{2}\overline{b}_1\alpha - \overline{b}_2\sigma^1 - \tfrac{3}{2}\overline{b}_3\alpha^{-1}\sigma^2 - \tfrac{1}{2}\sum_{k=3}^{\infty}\left(k+1\right)\overline{b}_{k+1}\alpha^{1-k}\sigma^k$$

After Equations (37)-(40) are combined with Equation(35) ,the sums of the coefficients of each power of σ on both sides equal zero, so the coefficients of σ^0, σ^1, σ^2, σ^k and σ^{-k} must satisfy the following requirements:

$$-\alpha a_0 + \left(1+\alpha^2\right)\alpha^{-1}b_1 - b_2\alpha^{-1} - \alpha\overline{c}_0 + \left(1+\alpha^2\right)\alpha\overline{c}_1 - \overline{c}_2\alpha^3 - \tfrac{3}{2}\alpha^3\overline{a}_3 - \left(1-3\alpha^2\right)\alpha\overline{a}_2$$

$$-\tfrac{1}{2}\left(3\alpha^3 - 3\alpha\right)\overline{a}_1 - \tfrac{1}{2}\alpha\overline{b}_1 = A_0 - \alpha C_2 \quad (41)$$

$$-a_1\alpha^2 + \left(1+\alpha^2\right)a_0 - b_1 - \overline{d}_1 + \left(1+\alpha^2\right)\overline{c}_0 - \overline{c}_1\alpha^2 - \overline{a}_2\alpha^2 - \tfrac{1}{2}\left(1-3\alpha^2\right)\overline{a}_1$$

$$+\tfrac{1}{2}\left(3\alpha^2 - \alpha^4\right)\overline{b}_1\alpha^{-2} - \overline{b}_2 = A_1 + \left(1+\alpha^2\right)C_2 \quad (42)$$

$$-a_2\alpha^3 + \left(1+\alpha^2\right)a_1\alpha - a_0\alpha - \bar{d}_2\alpha^{-1} + \left(1+\alpha^2\right)\bar{d}_1\alpha^{-1} - \bar{c}_0\alpha - \tfrac{1}{2}\bar{a}_1\alpha$$
$$+ \tfrac{1}{2}\left(3\alpha^3 - 3\alpha\right)\bar{b}_1\alpha^{-2} + \tfrac{1}{2}\left(3\alpha^2 - \alpha^4\right)2\bar{b}_2\alpha^{-3} - \tfrac{3}{2}\bar{b}_3\alpha^{-1} = A_2 - \alpha C_2 \tag{43}$$

$$-a_k\alpha^{k+1} + \left(1+\alpha^2\right)a_{k-1}\alpha^{k-1} - a_{k-2}\alpha^{k-1} - \bar{d}_k\alpha^{1-k} + \left(1+\alpha^2\right)\bar{d}_{k-1}\alpha^{1-k} - \bar{d}_{k-2}\alpha^{3-k}$$
$$+ \tfrac{1}{2}(k-3)\bar{b}_{k-3}\alpha^{3-k} + \tfrac{1}{2}\left(1-3\alpha^2\right)(k-2)\bar{b}_{k-2}\alpha^{1-k} + \tfrac{1}{2}\left(3\alpha^3 - 3\alpha\right)(k-1)\bar{b}_{k-1}\alpha^{-k} \tag{44}$$
$$- \tfrac{1}{2}\left(3\alpha^2 - \alpha^4\right)k\bar{b}_k\alpha^{-k-1} - \tfrac{1}{2}(k+1)\bar{b}_{k+1}\alpha^{1-k} = \alpha^k A_k \quad (k=3,4,5,...)$$

$$-b_k\alpha^{1-k} + \left(1+\alpha^2\right)b_{k+1}\alpha^{-1-k} - b_{k+2}\alpha^{-1-k} - \bar{c}_k\alpha^{k+1} + \left(1+\alpha^2\right)\bar{c}_{k+1}\alpha^{k+1} - \bar{c}_{k+2}\alpha^{k+3}$$
$$- \tfrac{1}{2}(k+3)\bar{a}_{k+3}\alpha^{k+3} - \tfrac{1}{2}\left(1-3\alpha^2\right)(k+2)\bar{a}_{k+2}\alpha^{k+1} - \tfrac{1}{2}\left(3\alpha^3 - 3\alpha\right)(k+1)\bar{a}_{k+1}\alpha^k \tag{45}$$
$$- \tfrac{1}{2}\left(3\alpha^2 - \alpha^4\right)k\bar{a}_k\alpha^{k-1} + \tfrac{1}{2}(k-1)\bar{a}_{k-1}\alpha^{k+1} = \alpha^k A_{-k} \quad (k=1,2,3,...)$$

According to Equations (1)-(2), it is clear that a_0, c_0 and C_2 are constants and have no effect on the stress distribution. To eliminate them, result of equations $(41)\times(1+\alpha^2) + (42)\times\alpha$ is written as

$$-a_1\alpha^3 - \tfrac{1}{2}\left(3\alpha^5 - 2\alpha - 3\alpha^3\right)\bar{a}_1 - \left[\alpha^3 + \left(1+\alpha^2\right)\left(1-3\alpha^2\right)\alpha\right]\bar{a}_2 - \tfrac{3}{2}\left(1+\alpha^2\right)\alpha^3\bar{a}_3 + \left[\left(1+\alpha^2\right)^2\alpha^{-1} - \alpha\right]b_1$$
$$+ \left(\alpha - \alpha^3\right)\bar{b}_1 - \left(1+\alpha^2\right)\alpha^{-1}b_2 - \alpha\bar{b}_2 + \left[\left(1+\alpha^2\right)^2\alpha - \alpha^3\right]\bar{c}_1 - \left(1+\alpha^2\right)\alpha^3\bar{c}_2 - \alpha\bar{d}_1 = \alpha A_1 + \left(1+\alpha^2\right)A_0 \tag{46}$$

And the result of Equations $(41) - (43)$ is written as

$$-\left(1+\alpha^2\right)\alpha a_1 + \tfrac{1}{2}\left(4\alpha - 3\alpha^3\right)\bar{a}_1 + a_2\alpha^3 - \left(1-3\alpha^2\right)\alpha\bar{a}_2 - \tfrac{3}{2}\alpha^3\bar{a}_3 + \left(1+\alpha^2\right)\alpha^{-1}b_1 - \tfrac{1}{2}\left(4\alpha - 3\alpha^{-1}\right)\bar{b}_1$$
$$-b_2\alpha^{-1} - \left(3\alpha^{-1} - \alpha\right)\bar{b}_2 + \tfrac{3}{2}\bar{b}_3\alpha^{-1} + \left(\alpha + \alpha^3\right)\bar{c}_1 - \bar{c}_2\alpha^3 - \left(\alpha^{-1} + \alpha\right)\bar{d}_1 + \bar{d}_2\alpha^{-1} = A_0 - A_2 \tag{47}$$

Because the complex stress functions $\phi(z)$ and $\psi(z)$ are convergent, four groups of constants a_k, b_k, c_k and d_k should close to zero on the condition of $k \rightarrow \infty$. Their values can be defined by Equations (28), (32), (44), (45), (46) and,47, and the solution is complete.

STRESS EXPRESSION OF TUNNEL SURFACE

On the condition that the supporting pressure (q0) is uniform or equal to k times the initial stress field, q(x, y) in Figure 3 can be written as

$$T_x = q\frac{x}{r}, \quad T_y = k'q\frac{y+h}{r} \tag{48}$$

where q is the pressure in the x-direction and equal to the initial pressure minus the supporting pressure at point (r, h) in the Z plane, K' equals the ratio of the stress in the y-direction at point (0,d) to the stress in the x-direction at point (r, h), r is the radius of the circular tunnel, and TxandTy are surface stresses in the X-direction and Y-direction. According to Equation (4), the force F(s)can be calculated by integrating along the stress boundary condition of the circular tunnel.

$$F(s) = i\int_{s_0}^{s}\left(T_x + iT_y\right)ds = \frac{i(1+k')q}{2}\int_{s_0}^{s}\frac{z+ih}{r}ds + \frac{i(1-k')q}{2}\int_{s_0}^{s}\frac{\overline{z+ih}}{r}ds \tag{49}$$

When a circular tunnel has a uniform radial force q, the method of Verruijt (1998) can be used to express itssurface stress under a bipolar coordinate system. In the bipolar coordinate system $z + ih = r\exp(i\beta)$ $ds = rd\beta$. On the supposition of $s_0 = 0$, where Equation(49) is combined with Equations (7) and (8) , the force F can be written as

$$F(s) = \frac{q(1+k)}{2}(Z + ih - r) + \frac{q(k-1)}{2}\left(\overline{Z - ih - r}\right) \tag{50}$$

$$= \frac{i(1+k)qh\alpha}{\left(1+\alpha^2\right)(1-\alpha\sigma)}[\alpha - \sigma + i(1-\alpha\sigma)] + \frac{i(k-1)qh\alpha}{\left(1+\alpha^2\right)(\sigma-\alpha)}[1 - \alpha\sigma + i(\sigma - \alpha)]$$

Then,Equation (36) can be rewritten as

$$F_1(\alpha\sigma) = (1-\alpha\sigma)(\sigma-\alpha)F(\alpha\sigma)$$

$$= \frac{i(1+k)qh\alpha}{\left(1+\alpha^2\right)}(\sigma-\alpha)[\alpha - \sigma + i(1-\alpha\sigma)] + \frac{i(k-1)qh\alpha}{\left(1+\alpha^2\right)}(1-\alpha\sigma)[1 - \alpha\sigma + i(\sigma - \alpha)] \tag{51}$$

$$= \frac{qh\alpha}{1+\alpha^2}\left\{\left[2k'\alpha + i(k'\alpha^2 - \alpha^2 - 1 - k')\right]\sigma^2 + \left(4i\alpha - 2k' - 2k'\alpha^2\right)\sigma + \left[2k'\alpha + i(k'-1-\alpha^2 - k'\alpha^2)\right]\right\}$$

And Equation (37) can be rewritten as

$$F_1(\alpha\sigma) = \sum_{k=-\infty}^{\infty} A_k\sigma^k$$

$$= \frac{qh\alpha}{1+\alpha^2}\left\{\left[2k'\alpha + i(k'\alpha^2 - \alpha^2 - 1 - k')\right]\sigma^2 + \left(4i\alpha - 2k' - 2k'\alpha^2\right)\sigma + \left[2k'\alpha + i(k'-1-\alpha^2 - k'\alpha^2)\right]\right\} \tag{52}$$

Comparing all the coefficients in Equation (52), it is clear that they are all equal to zero except for A_0, A_1 and A_2

$$A_0 = \frac{qh\alpha}{1+\alpha^2}\left[2k'\alpha + i(k'-1-\alpha^2 - k'\alpha^2)\right], \quad A_1 = \frac{qh\alpha}{1+\alpha^2}\left(4i\alpha - 2k' - 2k'\alpha^2\right)$$

$$A_2 = \frac{qh\alpha}{1+\alpha^2}\left[2k'\alpha + i(k'\alpha^2 - \alpha^2 - 1 - k')\right]$$

(53)

All the coefficients of the complex stress functions $F_1(\alpha\sigma)$, $\phi(z)$ and $\psi(z)$ can be defined. To guarantee the accuracy of the analysis, the number k should be greater than 100, and it is advisable to turn to a numerical method, such as by using Matlab.

DISCUSSION OF THE TWIN TUNNEL'S STRESS DISTRIBUTION

A twin circular tunnel's stress distribution is analyzed comparatively with the finite element method and an analytical method. The twin circular tunnel's model is shown in Figure 5. The surrounding rock is regarded as an elastic material under a plane strain condition, the elastic modulus is 6 GPa and the Passion ratio is 0.25. To simulate a deep tunnel stress field, the left boundary is fixed in the X-direction displacement, the bottom boundary is fixed in the Y-direction displacement, the surface boundary is the applied vertical stress, the right boundary is the applied horizontal stress, and gravity is not taken into account.
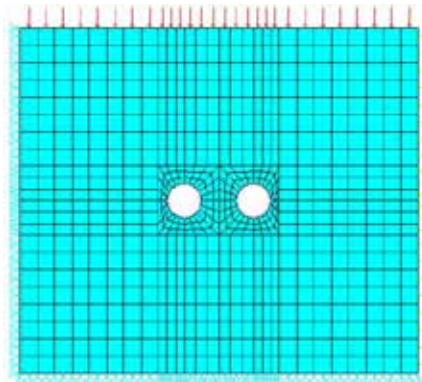
Fig. 5. Twin circular tunnel's model

To analyze different factors' influences on the twin tunnel's stress distribution, 4 deep-tunnel examples are applied under a vertical pressure q_v=1 MPa, as shown in Table 1, where the d/D is the ratio of twin tunnel's spacing distance to diameter. All are shown in Figure 6, and the expressed data are analytical results. Most of the tangential stressesare larger than the radial stresses around the tunnel, all the maximum stresses appear at the point of the middle rock wall, and the maximum stress of example (c) is 2.88 MPa and the largest.The spacing distance of the twin tunnel has a clear influence on its stress distribution. The tangential stress is larger at the left and right hances than at the vault and smaller than at the middle rock wall, so the stress concentration at the middle rock wall is the most

evident. Comparing examples (a) and (b), it is easy to conclude that increasing the supporting pressure leads to an increase in the radial stress and a decrease in the tangential stress, sothe supporting pressure is helpful to enhancing the tunnel's stability according to the rock's yield criterion.

Table 1. Deep-tunnel examples

Example	Stress coefficient	d/D	Supporting pressure
a	0.7	1.0	$0.5q_v$
b	0.7	1.0	$0.1q_v$
c	0.7	0.5	$0.1q_v$
d	1.0	1.0	$0.1q_v$
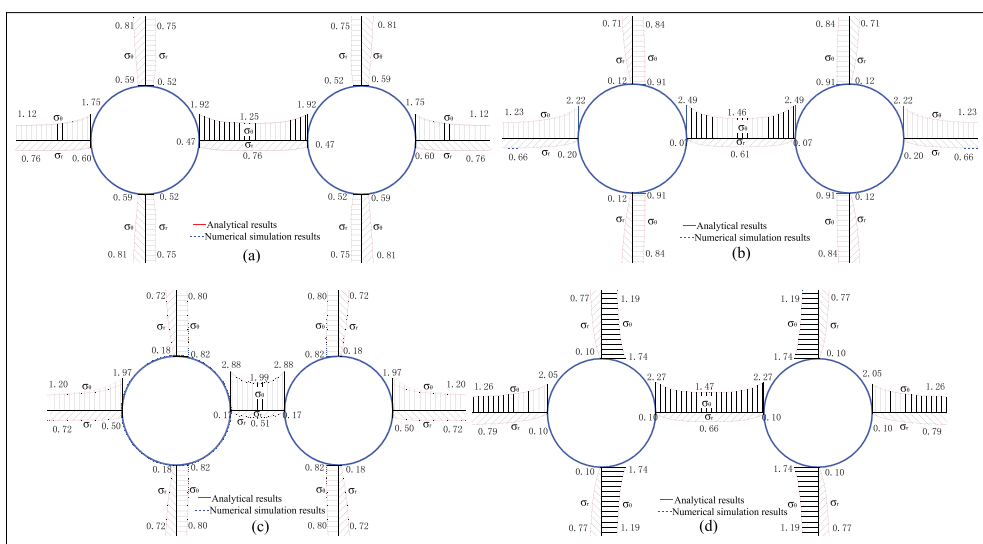
Fig. 6. Twin tunnel's stress distribution

When the stress coefficient of example (b) increases from 0.7 to 1, it becomes example (d), which reduces the maximum stress from 2.49 MPa to 2.27 MPa, and reduces the hance's tangential stress from 2.22 MPa to 2.05 MPa, but increases the vault's tangential stress from 0.91 MPa to 1.74 MPa. Comparing the analytical results with the numerical results, the two methods' data are very consistent with each other, but the differences in the stress distributions are most evident at the left and right hances, particularly when the spacing distance is very small, as shown in Figure 6(c).

Thefour examples' tangential stress distributions at the tunnel boundary are shown in Figure 7, and the tangential stress is calculated with σ_x, σ_y and τ_{xy} according to the plane stress formula $\sigma_\theta = \sigma_x\cos^2\theta + \sigma_y\sin^2\theta + 2\tau_{xy}\sin\theta\cos\theta$. It is clear that all the maximum tangential stresses appear at middle rock wall and all the minimum tangential stresses appear at the vault, except in example (d), and the numerical results show the same trends. The only difference between examples (a) and (b) is the supporting pressure, which shows that the supporting pressure has a clear influence on the tangential stress distribution. Upon increasing the supporting stress from $0.1q_v$ to $0.5q_v$, the tangential stresses at the hance, vault and middle rock wall decrease from 2.22MPa, 0.91MPa and

2.49MPa to 1.75MPa, 0.59MPa and 1.92MPa, respectively. When the spacing distance of example (b) decreases from 1d to 0.5d, the tangential stresses at the hance and vault decrease to 1.97MPa and 0.82MPa,respectively, but at the middle rock wall, it increases to 2.88MPa.The stress distribution differencearound the tunnel's boundary in example (d) is the smallest in the 4 examples. Comparing examples (b) and (d), it may be concluded that a lower stress coefficient leads to a higher stress concentration. The most evident difference between the analytical data and numerical data appears at the hance in example (c), and the differences in the other examplesare small.
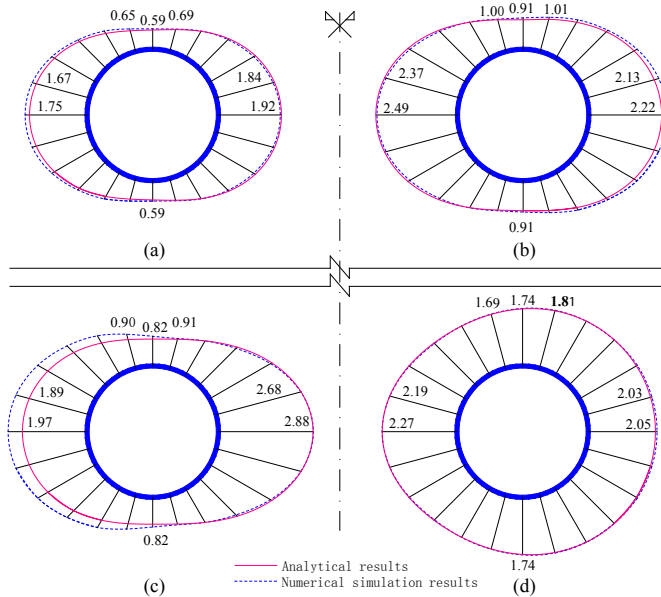
Fig. 7. Twin tunnel's tangential stress distribution at boundary

Judging from the twin tunnel's stress distribution, the most attention should be placed on the middle rock wall where the maximum stress appears. The following will analyze the influence of d/D, q_h/q_v and the supporting pressure q_0 on the stress concentration at the middle rock wall.

With d/D=0.5, the influences of q_0 and k' on the stress concentration are shown in Figure 8. The supporting pressure and stress coefficient are helpful to reduce the stress concentration.When the supporting pressure is zero andthe stress coefficient increases from 0.5 to 1, the stress concentration factor falls from 3.17 to 2.97. When the supporting pressure decreases from 50% q_v to zero with k'=1, the stress concentration factor increases from 1.97 to 2.94. Hence, the supporting pressure hasa more significant influence on the stress concentration, and the linear relationships between the stress concentration and the two factors are obvious.

When the stress coefficient equals 0.8, the influences of q_0 and d/D on the stress concentration are shown in Figure 9. It is clear that d/D's influence on the stress concentration is stronger than that of the supporting pressure. The stress concentration increases rapidly with the decrease in d/D. When the supporting pressure is zero and d/D falls from 1.5 to 0.1, the stress concentration factor changes from 2.33 to 4.69. According to Figure 8 and Figure 9, it is clear that the spacing distance hasthe greatest influence on the stress concentration.
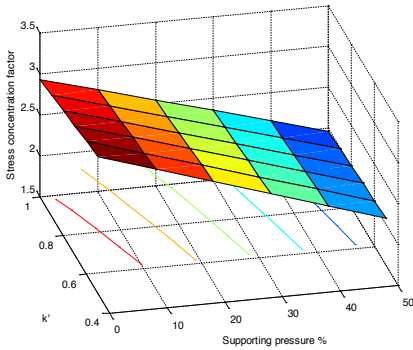
Fig. 8. Influence of q_0 and k' on stress
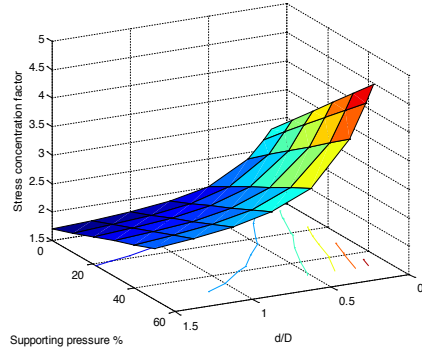
Fig. 9. Influence of q_0 and d/D on stress

With no supporting pressure, theinfluences of k' and d/D on the stress concentration are shown in Figure 10. Compared with the influence of d/D , the influence of k' on the stress concentration is minor. It is interesting to observe that thestress concentration factor slowly decreases with the spacing distance's reduction in the small region of a stress coefficient below 0.7 and d/D below 0.25, and this is worthy of discussion.

To verify that the results are reasonable, the finite element method isapplied to analyze the stress concentration for comparison with the analytical method, as shown in Figure 11, where k1 is the conditions that d/D is variable with k'=1 and $q_0=0.2q_v$; k2 is the conditions that d/D is variable with k'=0.8 and q_0=0; and k3 is the conditions that q_0 is variable with k'=1 and d/D=0.5. It is easy to conclude that when d/D exceeds 0.25,the analytical results have good agreement with the numerical data, but the difference between the analytical and numerical data o may increase when d/D is below 0.25 and k' is below 0.7. When the spacing distance is very small, the analytical results based on the superstition method may fail to guarantee the calculation accuracy(Tran-Manhet al., 2015).
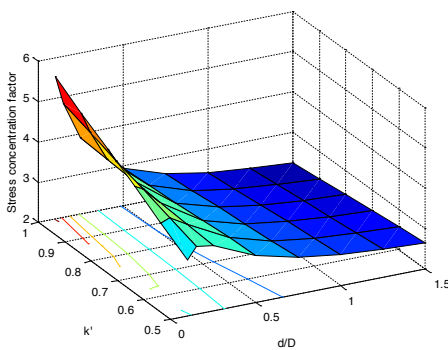
Fig. 10. Influence of d/D and k' on stress
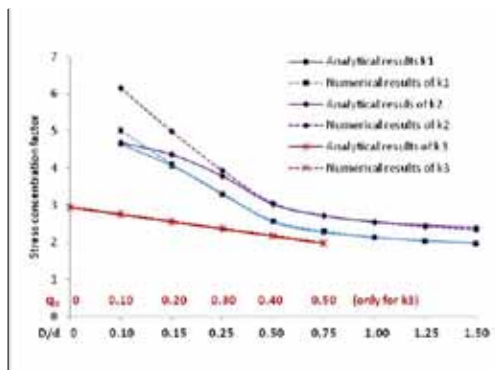
Fig. 11. Stress concentration comparison

CONCLUSIONS

Based oncomplex variable theory and the superposition principle, an elastic solution fora deep twin tunnel's stress in a homogeneous and isotropic rock subjected to non-uniform stress is presented. Analyzing the influences of the ratio of the spacing distance to the tunnel's diameter, the stress coefficient and the supporting pressure on twin tunnel's stress distribution, it is easy to conclude that the maximum stress appears at the middle rock wall,the spacing distance has the greatest influence on the stress concentration and the secondstrongest influence is the supporting pressure. Comparing the analytical method with the finite element method, the greatest differences between the two methods' results appear at the left and right hances, so the two methods' results are very consistent with each other. However, the twin tunnel's spacing distance and the stress coefficient have an influence on the results' accuracy. In the small region where the spacing distance is less than 0.25 time the tunnel diameter and the stress coefficient is below 0.7, the difference between the analytical data and numerical data may become obvious, and it is worth paying attention to.

ACKNOWLEDGMENTS

REFERENCES

Bobet A. 2016. Deep lined circular tunnels in transversely anisotropic rock: Complementary Solutions. Rock Mechanics and Rock Engineering, **49**:3817-3822.

Carranza-Torres C, Rysdahl B, Kasim M. 2013. On the elastic analysis of a circular lined tunnel considering the delayed installation of the support. International Journal of Rock Mechanics and Mining Sciences, 61:57-85.

CB Kooi, AVerruijt, 2001. Interaction of circular holes in an infinite elastic medium.Tunnelling and underground space technology, **16** (1):59-62.

Exadaktylos G, Stavropoulou M. 2002.A closed-form elastic solution for stresses and displacements around tunnels. International Journal of Rock Mechanics and Mining Sciences, **39**(7): 905-916.

Fu J, Yang J, Yan L, Abbas, S-M. 2015. An analytical solution for deforming twin-parallel tunnels in an elastic half plane. International Journal for Numerical and Analytical Methods in Geomechanics, **39**(5):524-538.

KargarA R, Rahmannejad R, Hajabasi M A. 2014. A semi-analytical elastic solution for stress field of lined non-circular tunnels at great depth using complex variable method. International Journal of Solids and Structures, **51**(6):1475-1482.

Ling C B. 1948. On the stresses in a plate containing two circular holes [J]. Journal of Applied Physics, **19**(1):77-82.

Li S-C, Wang M-B. 2008. An elastic stress–displacement solution for a lined tunnel at great depth. International Journal of Rock Mechanics and Mining Sciences, **45**(4):486-494.

Lü A-Z, Zhang L-Q, Zhang N. 2011. Analytic stress solutions for a circular pressure tunnel at pressure and great depth including support delay. International Journal of Rock Mechanics and Mining Sciences, **48**(3):514-519.

Park, K. 2004. Elastic Solution for tunneling-induced ground movements in clays. International Journal of Geomechanics, **4**(4):310-318.

Pender, M.1980. Elastic solutions for a deep circular tunnel.Geotechnique, **30**(2):216-222.

Strack E, Verruijt A.2002. A complex variable solution for a deforming buoyant tunnel in a heavy elastic half-plane. International Journal for Numerical and Analytical Methods in Geomechanics, **26**(12):1235-1352.

Su F,Chen F-Q, Shi Y-Z, 2012. Analytic continuation solution of deep twin-tunnels, Chinese Journal of Rock Mechanics and Engineering, **3**1(2):365-374(in Chinese).

Sulem, J., Subrin, D. & Monin, N. 2013. Semi-analytical solution for stresses and displacements in a tunnel excavated in transversely isotropic formation with non-linear behavior. Rock mechanics and rock engineering, **46**(2): 213-229.

Tran-Manh H, Sulem J, Subrin D. 2015. Interaction of circular tunnels in anisotropic elastic ground. Géotechnique, **65**(4):287-295.

Verruijt A. 1998. Deformations of an elastic half plane with a circular cavity. International Journal Of Solids And Structures, **35**(21):2795-2804.

Wang, S-L.,Wu, Z-J., Guo, M-W. & Ge, X-R. 2012.theoretical solutions of a circular tunnel with the influence of axial in situ stress in elastic–brittle–plastic rock. Tunnelling and Underground Space Technology, **30**:155-168.

Yan L, Yang J-S, Liu B-C, 2011. Stress and displacement of surrounding rock with shallow twin-parallel tunnels. Chinese Journal of Geotechnical Engineering, **33**(3):413-419(in Chinese).

Zhang L-Q, Yang Z-F, Lü A-Z. 2000. Analysis study on displacement field of surrounding rocks of two parallel tunnels with arbitrary shapes and its application to back-analysis of displacement[J]. Chinese Journal of Rock Mechanics and Engineering, **19**(5):584-589(in Chinese).

Zhao, G. & Yang, S. 2015. Analytical solutions for rock stress around square tunnels using complex variable theory. International Journal of Rock Mechanics and Mining Sciences, **80**:302-307.